International Journal of Current Research and Applied Studies, (IJCRAS)

ISSN: 2583-6781

available at https://ijcras.com/

Volume 4 Issue 2 Mar-Apr 2025, Page 17-36

To cite this article: Desiran Sembiring, Daud Surbakti and Ab Saman (2025). FAILURE ANALYSIS OF WATER TUBE BOILER: CASE STUDY AT TEXTILE PROCESSING PLANT, International Journal of Current Research and Applied Studies (IJCRAS) 4 (2): Article No. 116, Sub Id 199

FAILURE ANALYSIS OF WATER TUBE BOILER: CASE STUDY AT TEXTILE PROCESSING PLANT

Desiran Sembiring[1]*, Daud Surbakti[2] and Ab Saman[3]

[1]Lecturer Faculty of Mechanical Engineering, Institut Sains Tekhnologi Nasional (ISTN) Jakarta, Indonesia.

[2]Lecturer Faculty of Mechanical Engineering, Universitas Mpu Tantular Jakarta, Indonesia.

[3]Lecturer Faculty of Mechanical Engineering, Universiti Teknologi Malaysia (UTM) Skudai, Johor Baru, Malaysia.

DOI : https://doi.org/10.61646/IJCRAS.vol.4.issue2.116

ABSTRACT

A boiler is a closed vessel where the combustion heat is transferred to the water until hot water or steam is formed. The failure occurred on the boiler water tubes at the textile processing plant, after an eight-year operation, which experienced damage like water tubes rupture in position at the bottom of the furnace boiler. In this position, the boiler water tubes directly received heat from burning coal. Damage occurred on the water tubes starting from a permanent form change until the rupture of the box (water tube boiler). The testing results of the boxes' chemical composition, the boiler, failed and the matter degraded, such as; C, Mn, Ni, Cr, Ti, Mo, and Cu, which will reduce the physical and mechanical properties of the material of the tubes. Analysis of the results obtained by visual observation showed the tube's box's fish mouth, and this indicated overbooking on the tubes. The test results showed that the hardness of tubes in the damaged tubes has lower hardness than undamaged tubes. Under these conditions, the damaged tubes experienced softening (annealing). This is corroborated by the testing results of the tensile strength, which indicated that the tensile strength of the damaged tubes decreased compared to the undamaged tubes. Microstructures tubes' microstructures ruptured tubes experienced a

change from ferrite and pearlite became pearlite spheroidizing at grain boundaries. This differs from the microstructure on the intact tubes' material, namely in the form of ferrite pearlite with a fine grain.

Keywords: boiler, tubes, failure, rupture (burst), microstructure

INTRODUCTION

A boiler is a closed vessel where the combustion heat is transferred to the water until hot water or steam is formed. The boiler's important components are a furnace, the chamber, heat exchangers and control system, and safety accessories. The right composition in mixing the fuel and air in the combustion chamber will produce perfect combustion. The combustion heat heats the boiler tubes in which water transfers the heat into water vapor through the heat exchanger system. The steam with certain pressure is used to give the vapor to a dying jet system and dye textile products. The existence of heat, pressure, abrasive and corrosive environment that experienced continuously for a long time leads the initial failure of the water tube boiler [1–3]. A failure happened on the water tubes at the textile processing plant. The boiler operated 24 hours/day in a full year, and an overhaul is scheduled every two years, inclusive of cleaning the boiler tubes. The fireside was cleaned with a mechanical system, and the waterside was cleaned with a chemical. Boiler feed-water is taken from groundwater. The feed-water system used an installation water softener system. Table 1 shows the specifications of boilers.

Nevertheless, the boiler is not equipped with a de-aerator tank. Water from the softener tanks directly entered into the daily tank boiler and onward as boiler feed water on the installation of water softener boiler feed-water at controlled quality, with chemicals to get the quality boiler feed water which meets the standard boiler feed water, especially which is demanded, such as water pH is maintained between 6 - 8. The boilers use solid fuel in low-calorie coal, working at a maximum pressure of 15 kg/cm2. During the 8-year operation, the boiler had rupture on the tubes at the bottom of the furnace boiler, where the tubes directly received the heat from the combustion of coal fuel. The visible damage on the tubes started from the change of permanent forms until bulging and rupture of the tubes, so that this required boiler shutdown to replace the tubes. Fig 1 illustrated the general water tube boiler system in the plant and the location of the failure.

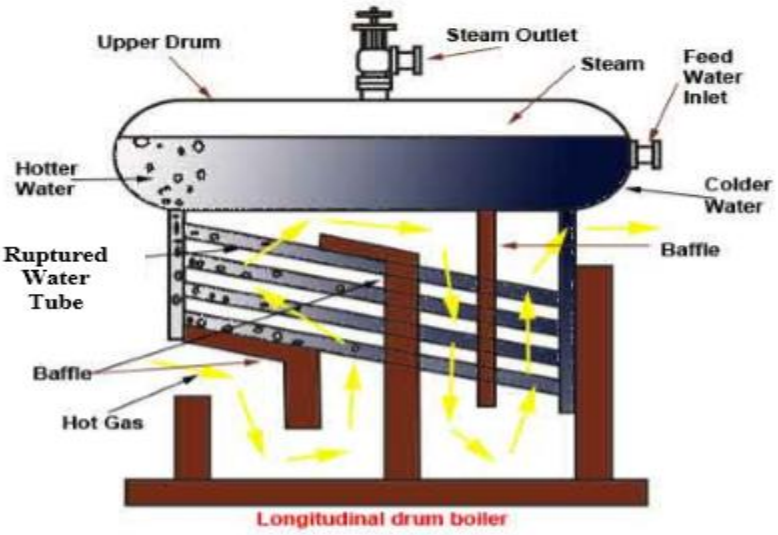

Fig. 1 - Ruptured tubes position

The investigation was carried out by the failure analysis method through several examinations and destructive tests to determine the cause of failure, namely visual observation, chemical composition analysis using spectroscopy, hardness testing using a *micro-Vickers tester,* and microstructure testing using optical microscopy and *scanning electron microscopy* (SEM). The observations of failure characteristics are as follow: on a used tube, there is a local thinning, especially at the location of the walls of ruptured tubes as a result of tangential stress. From the results of the evaluation of the failure of the boiler tubes, it was caused by the occurrence of excessive heat *(overheating)* due to the deposited water crust deposited *(scale deposits)*, which prevented the heat transferring process. After a visual observation of data coupled with information obtained from a boiler operator, the possible cause of failure in the tubes are as follows:

Table 1 - Boiler Specification Data

Merk	: Unknown
Type	: Water Tube Boiler
Manufactured Year	: 2012
Maximum Pressure	: 15 kg/cm^2
Steam Temperature	: Unknown
Fuel	: coal (low calorie)

This study aims to identify the root causes of the significant reasons for the water tube components failure and to use this information as assessment material for implementing preventive actions.

2. METHODOLOGY

When there is a failure in the boiler tubes, especially on water tubes, observation and collection of samples and evidence are conducted to lead to the cause of a failure. Data retrieval in the field was carried out

through interviews with operators, visual observation, macroscopic observations, microscopic observation, and collecting of operating data and specifications from the operational boiler system at a textile processing plant. Research on finding the cause of the tube's failure at the textile processing plant was made by the method of failure analysis approach.

2.1 Observation and Study of Literature

When there is a failure in the boiler tubes, especially on water tubes, observation and collection of samples and evidence are conducted to lead to the cause of a failure. Data retrieval in the field was carried out through interviews with operators, visual observation, macroscopic observations, microscopic observation, and collecting of operating data and specifications from the operational boiler system at a textile processing plant. Fig. 2 shows the flow-sheet of inspection and testing of the damaged tubes.

2.2 Preparation of Specimens

After taking some samples of the failed water tube, the specimen preparation process was carried out according to the laboratory's testing standards. Specimen preparation includes cutting, mounting, grinding, and polishing.

2.2.1. Chemical Composition Specimens Preparation

Methods of spectroscopy are used to examine the composition of chemical elements in the samples from the tubes, which can then be compared with a standard tube specification for the boiler or the tubes that do not fail (intact). "Comparing to some intact tubes is to see some happening changes" such as the first change in physical properties; chemical composition, grain size, and phases. While the results of these changes will continue to change into mechanical properties such as hardness, tensile strength, corrosion, creep, etc.

2.2.2. Hardness Test Specimens Preparation

Hardness Observation on failure analysis using the method of micro-Vickers with diamond indent or refers to the standard ASTM E92 [17] to determine the differences and changes in hardness in the samples of boiler tubes that have failed and standard tubes material to the boiler or in tubes that do not experience failure (intact). The test is carried out at three examination points, from the one that is close to the ruptured part until the farthest part and the intact ones.

2.2.3. Microstructure Specimens Preparation

Microscopic observation with the metallographic method was conducted to analyze the morphology and distribution of grains and phases formed in the sample of tubes, which failed to refer to the ASM Handbook Volume 9 (2004) [15]. Microstructure observation on tube samples used scanning electron microscopy (SEM) JEOL JSM 6390 A technique of backscattered electron and mapping.

2.3. Testing of Specimens

After the tube samples' cutting process in a close position to the damaged area *(Burst)*, the next stage is

testing. The tests performed include visual inspection of the ruptured area, micrographic inspection, the examination of the microstructure, hardness testing, the tensile strength and chemical composition analysis of the tubes, using *optical emission spectrometry (OES)*, and testing the composition of the crust/scale deposit with the *Energy Dispersive X-ray Fluorescence (EDXRF)* method.

A visual inspection was carried out to identify the location of the damage, the form of the damage, and to determine the initial area of the cause of the damage, which will be selected for further examination. This method was done by checking the conditions and contours of the damaged area accurately and then documented it with a digital camera.

Along with the visual examination, the macro graphic examination used a stereomicroscope to identify early damage to the leaking or ruptured area's surface so that the area can be exposed at a higher magnification than the visual examination. Hence clearer information can be obtained from the results of the macro graphic examination. The macro graphic examination was carried out at a magnification of 12x. Macro graphic examination refers to ASTM E 340-00. The metallographic examination used an optical microscope performed to examine the initial damage in more detail. The surrounding areas of the damage were associated with microstructure and changes during the operation process. Besides, a metallographic examination was performed to check for the presence of *micro void*, micro-cracks, or other micro-defects that may be present and have an effect as a cause of damaged and leaking tubes. The results are then documented with a digital camera.

The preparation of metallographic specimens refers to the ASTM E 3-01 standard, which includes several stages, including cutting metallographic specimen material in the form of water tube material (water tube boiler) using a hand grinder. The process of forming the test sample using techno vit or acrifix powder mixed with a specific ratio of hardening liquid, where the liquid mixture becomes hard and takes ± 1 hour. The grinding/sanding process uses Struers hand grinding machines and silicon carbide (SiC) emery paper with various roughness, namely a combination of 80,120, 220, 360, 500, 600, 800, 1000, and 1200 mesh. The washing process used 95% alcohol and then dried it with a blow dryer. The process of polishing/polishing test tube samples used diamond paste form. Furthermore, the tube test samples' micro etching process was carried out, which refers to the ASTM E 407-01 standard where the solution used is Nital 2%.

Testing the tubes' material hardness was performed around the damaged area to find out the possibility of hardness value changes probably causing the damage due to softening (annealing) or the contrary hardening happened (quenching). The used method is indented *Hardness Vickers* (HV) refers to ASTM E 92. The load used was five kgf using a diamond indenter with an angle of 136°. Analysis of the tubes' chemical composition that failed and standard tube materials for the boiler or the tube's material that does not fail (intact) using *optical emission spectrometry (OES)*. The examination was carried out to determine the type of alloy steel so that it is easier to choose a substituting material, as well as to find out changes in composite and process. Comparing the chemical composition of the tubes' material that failed and the

tube's material that does not fail (intact) to evaluate the likelihood of degradation of the material's composition. Chemical composition examination refers to Standard ASTM A213.

Preparation of the test sample on the tubes' chemical composition using grinding and sanding to rudeness 40 CCW. SEM analysis was carried out on the surface of the damaged area to examine the leak's shape in more detail and find other evidence that may be present and contribute to the initial failure. Analysis of corrosion product or crust/scale deposit used method of Energy Dispersive X-ray Fluorescence (XRF) to check for the presence of suspicious elements such as aggressive ions or corrosive ions, which may contribute to further damage.

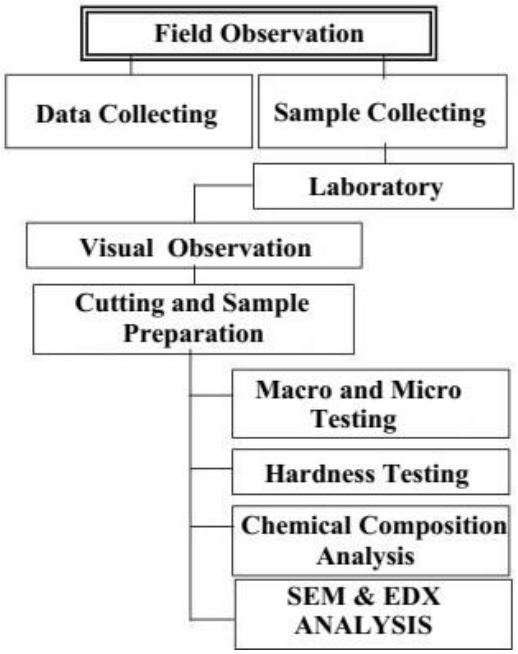

Fig. 2 - The flow-sheet inspection and testing of the damaged tubes

3. RESULTS AND DISCUSSION

3.1. Visual Observation

The visual observation of Fig. 3 showed that the condition of tubes experienced a bulging before it burst (ruptured).

(a) **(b)**

Fig. 3 - Visual inspection and test position of boiler tubes. (a) Macro graphical tubes that suffered damage leaks (burst) part of the tubes on the fireside; (b) The macro graphic of the surface of the water tube boiler on the waterside experienced a burst.

There is a build-up of combustion scale/deposit while on the inside, there is a white scale, expected as silica. From the results of these visual observations, it is also seen that there are corrosion products throughout the fireside of the tubes in Fig. 3(a), which is brownish yellow and rough. The presence of corrosion products indicates a reaction of fuel gas and is exposed to temperatures above normal that should be accepted by the tubes' material. Stacking scale deposits in the area burst had hot spots that reduce their thickness because of the oxide reaction or corrosion.

Where as in Fig. 3(b) the surface of the boiler tubes on the waterside that experienced burst. A build-up of scale/combustion deposit is quite thick and layered with different colors. The precipitate that formed stuck to the tubes' surface is brownish-black like iron oxide, which occurred due to the high temperatures exposed in the air, while the scale layers/sediment preconceived white, thick, and hard thought to be a compound of silica produced by water.

3.2.Chemical Composition Testing

Testing the chemical composition of tubes' material experiencing a rupture, and intact boiler tubes and Standard Tubes ASTM A213 T12A are shown in Table 2. The results of the chemical composition test of table 2 show that the tubes' material failed and the tube's material that does not fail (intact). Some degraded elements, such as; C, Mn, Ni, Cr, Ti, Mo, and Cu, will reduce the physical and mechanical properties of the tube's material. Compared with ASTM A213 T12A material standards with tubes' material that does not fail (intact) have different conditions, especially on the elements C, Cr and Mo, which tend to be higher. Material specification of ASTM A213 Grade T12 [10] is low carbon steel, which has good creep resistance, high ductility, low hardness, and wieldable [7]. Table 2 also shows the elements of chromium and molybdenum on the results of the chemical composition of intact tubes, where the numbers are on the outside of the allowable range of compositions. The chromium element is a constituent element that mainly functions to raise the corrosion resistance, toughness and stability at high

temperatures. Also, the chromium element also plays a very important role in the formation of hard carbide compounds, so that it will increase the hardness of the steel [8] [9].

Table 2 - Chemical composition test results

Matter	Water Tube	Intact Water Tube	ASTM-A213-T12A
	%		
C	0.0887	0.091	0.05-0.15
S	0.0107	0.0123	Maximum 0.026
P	0.0033	0.0151	Maximum 0.025
Si	0.0061	0.1954	Maximum 0.50
Mn	0.4012	0.5062	0.30-0.61
Ni	0.071	0.0986	-
Cr	0.009	0.1443	0.80-1.25
V	0.0573	0.0037	-
TI	0.0035	0.0278	0.0278
Al	0.024	0.036	0.0235
Mo	0.027	0.053	0.44-0.65
Cu	0.105	0.1769	-
Nb	0.0008	0.0018	-
Fe	Balance	Balance	Balance

3.3.Hardness and Tensile Test

Hardness testing is carried out on the damaged area and the undamaged area according to figures 4 and 5, where each region gets data 3 times. The comparison of hardness testing of the damage tubes and intact tubes showed that the hardness decreased in areas far from the burst around 117-105 HV, but the hardness increased in the burst area 117 - 119 HV due to a change in the ferrite-pearlite phase into pearlite spheroidization (Fig. 14). However, when compared to standard ASTM 213 material, its hardness value is 178 HV. This is away different from the intact water tube boiler material. It means that the tube's material used has a hardness value of 117 HV. Table 4 showed the tensile test result of the specimens. The tubes' overall tensile strength is reduced due to a softening process caused by annealing temperature > 550 °C. The tensile strength decreased by approximately 11.5% and a yield strength decline of about 16.25% as well as the elongation decreased by around 14.8%. However, when compared with the standard ASTM 213 material, it is not much different from the intact tube material, meaning that the tube material which was chosen and used was good.

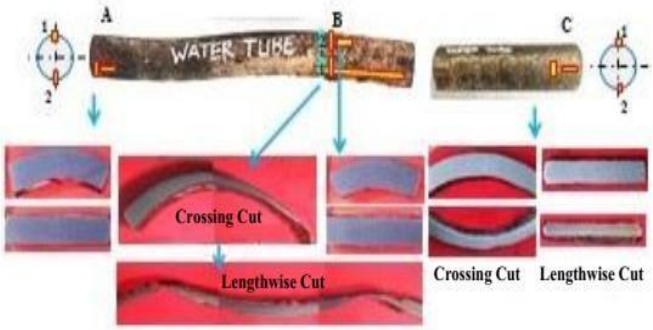

Fig 4. Sample collecting position for hardness test on tubes

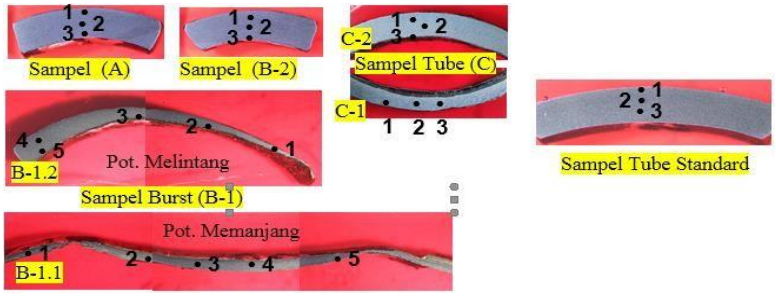

Fig. 5 - Position of the hardness test on a ruptured water tube boiler

Table 3 - The material hardness value of tubes

Water Tube							Intact Water Tube
No	Sample A	Sample B-1.1	Sample B-1.2	Sample B-2	Sample C-1	Sample C-1	
1	104	99.5	107	104	97	120	118
2	107	113	107	105	107	120	117
3	107	118	103	107	112	117	118
4	-	106	105	-	-	-	-
5	-	101	114	-	-	-	-
Average	106	107	107	105	105	119	117

Tool Name : Frank Finest
Testing Method : Hardness Vickers (HV)
Load : 5 Kgf
Identor Angle : 136°

Table 4 - Tensile test results for boiler tubes and standard tubes

Sample	σy (N/mm^2)	σu (N/mm^2)	ε (%)	Hardness
Intact Tubes	333-307 (320)	434-420 (427)	26-28 (27)	117
Broken Tubes	2247-289 (268)	371-385 (378)	22-24 (23)	105 - 119

3.4. Water Crust Deposit Analysis

Based on the macro-observations presented in Fig. 6, it is clear that there was a deposit of water crust (scale) inside the tube. The existence of the crust can disrupt the heat transfer mechanism of the system and make the tube overheats. Moreover, XRF analysis (Fig.7 and Table 5) and SEM-EDS analysis (Fig.8) was subjected to find out the chemical composition of the crust. The results present the elements of the crust that the majority of elements include oxygen, sulfur, sodium, silica, magnesium, and calcium. The data confirm that the crust strongly suspected is an oxide compound.

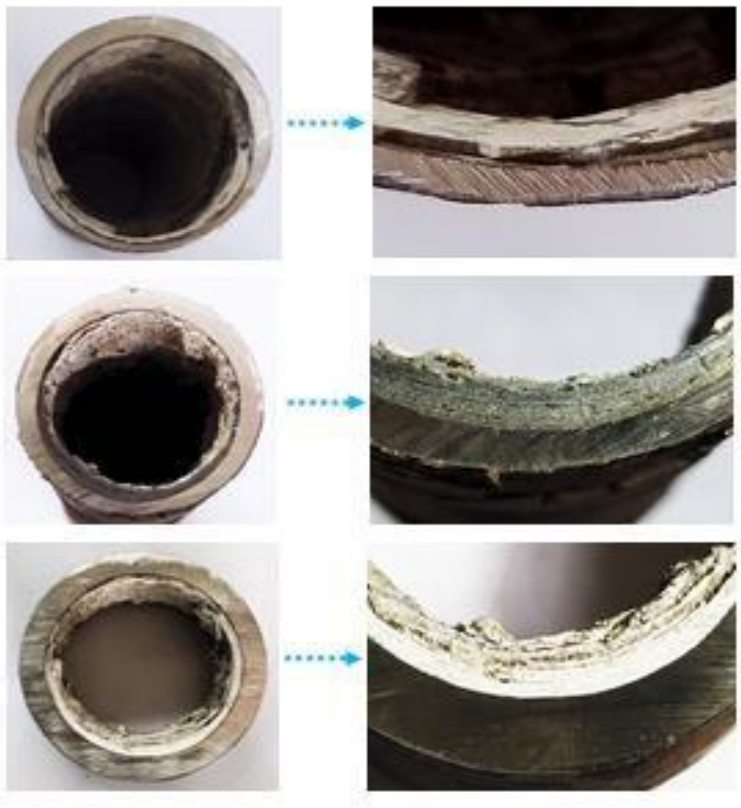

Fig. 6 - Deposits on the surface of boiler tubes at the waterside

From the results of XRF testing, as shown in Table 5 and Figure 8, it can be seen that the dominant elements in the water tube boiler are solid which tends to form deposits of calcium carbonate ($CaCO_3$), calcium sulfate ($CaSO_4.2H_2O$), magnesium carbonate ($MgCO_3$) and strontium deposits. Sulfate ($SrSO_4$)

has a low forming intensity beside other scale deposits, such as iron carbonate ($FeCO_3$), iron sulfide (FeS).

The results of the examination of corrosion products using EDS as shown in Fig.8, showed that the dominant elements which are corrosive elements that accelerate the damage of the material. The existing elements considered from the combustion of fuel in the boiler system reacted with air to form oxide compounds [14] and become corrosion products in the form of a crust attached to the tubes' outer surface.

Table 5 - Composition of XRF water tube crust

FE (%)	Zn (%)	Al (%)	Si (%)	P (%)	S (%)	Cl (%)	Na (%)	Mg (%)
38.7	0.011	0.341	24.823	0.468	0.456	0.342	4.634	4.909
K (%)	Ca (%)	Sc (%)	Ti (%)	Cr (%)	Mn (%)	Ni (%)	Cu (%)	Sr (%)
0.246	24.319	0.067	0.027	0.099	0.251	0.019	0.076	0.177

Sample ID: Water Tube Crust Experiment name: SMART-Element Measurement finished: 26/11/2020

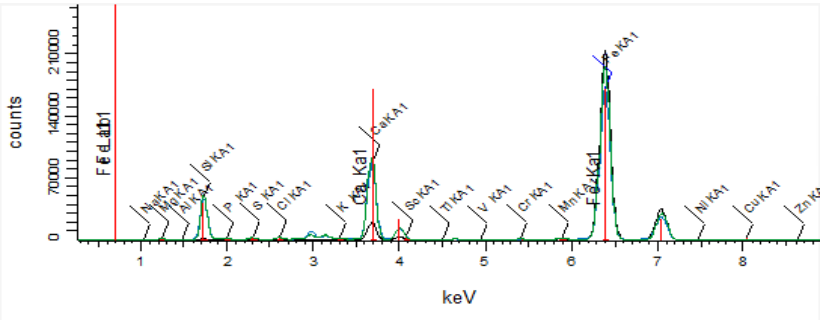

Fig. 7 - XRF results on the surface of the crust in a water tube (water tube boiler)

Table 6 - Quality feed water table

Parameter	Unit	Limit Controlling
pH	Unit	10.5 – 11.5
Conductivity	Mmhos.cm	5000, max
TDS	Ppm	3500, max
P-Alkalinity	Ppm	-
M-Alkalinity	Ppm	800, max
O-Alkalinity	Ppm	2, 5 x Si O2. Min
Hardness	Ppm	-
Silica	Ppm	150, max
Iron	Ppm	2, max
Phosphate Residual	Ppm	20 – 50
Sulfite Residual	Ppm	20 – 50
pH Condensate	Unit	8.0 – 9.0

The results of the examination of the corrosion products in the form of scale are then carried out using

the Energy Dispersive Spectroscopy (EDS).

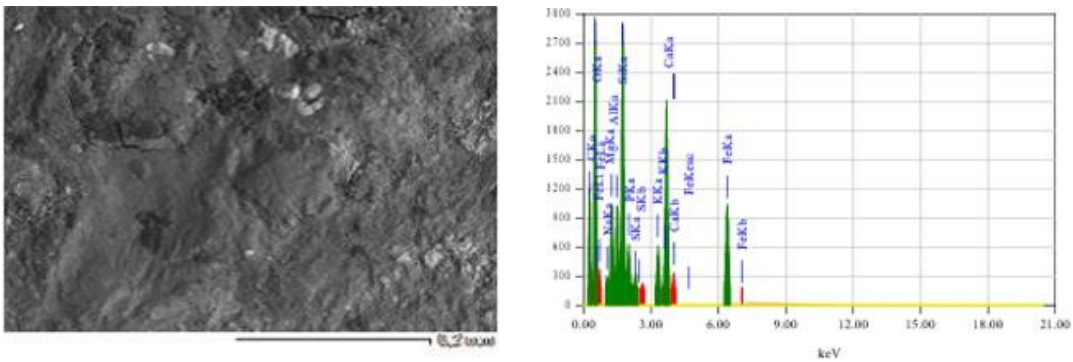

(a) **(b)**

Fig. 8 - Results of SEM-EDS crust on the surface boiler tubes *at* a fireside. (a) SEM results on the surface of the tubes on the fireside; (b) EDS results in the crust on the surface of the tubes on the fireside

3.5.Microstructure Observation

The microstructural test was conducted at two points: the damaged areas and areas that did not damage, as shown in Figure 9. Microstructure and hardness tests were conducted on two points, namely the area of tubes that were damaged and the area of tubes that were not, as shown in Fig. 9a and 9b. At Location, A Fig. 9 b), the microstructure with lengthwise cut (locations 1, 2 and 3) was in the form of ferrite (white) and pearlite, which transformed into a dispersion of pearlite at grain boundaries. At Location A, Fig. 10, the microstructure with lengthwise cut (locations 1, 2 and 3) was ferrite (white) and pearlite, which transformed into spheroidization of pearlite at grain boundaries. At Location B Figure 11, the microstructure with crossing cut (locations 1, 2, 3 and 4) was ferrite (white) and pearlite which transformed into spheroidization of pearlite at grain boundaries. At Location B Fig. 12, the microstructure (burst location) of sample 2 with crossing cut (1 and 3) was ferritic and at location 2 was ferrite-pearlite which transformed into pearlite spheroidization at the grain boundaries. At Location B Fig. 13, the microstructure samples (burst location) with crossing cut (1, 2 and 3) were ferrite and pearlite spheroidization at the grain boundaries. At Location B Fig. 14, the microstructure (burst location) of the sample 2 with lengthwise cut (1, 2 and 3) was in the form of ferrite and pearlite spheroidization at the grain boundaries. At Location C Fig. 16, the crossing cut microstructure (1, 2 and 3) was in the form of ferrite and pearlite spheroidization at the grain boundaries. At Location C Fig. 17, the microstructure of sample 1 had a lengthwise cut that extended outside in the form of ferrite and the middle (2) and the inside (3) in ferrite and pearlite spheroidization at the grain boundaries. At Location C Fig. 18, the microstructure of sample 2 with crossing cut (1) was in the form of ferrite and the middle (2) and the inside (3) was in the form of ferrite and pearlite spheroidization at the grain boundaries. At Location C Fig. 19, the microstructure of the sample 1 had a lengthwise cut extending outside in the form of ferrite and the middle (2) and the inside (3) in the form of ferrite and pearlite spheroidization at the grain boundaries. The phase degradation indicate that the tube has been experienced relatively high temperatures for a long time.

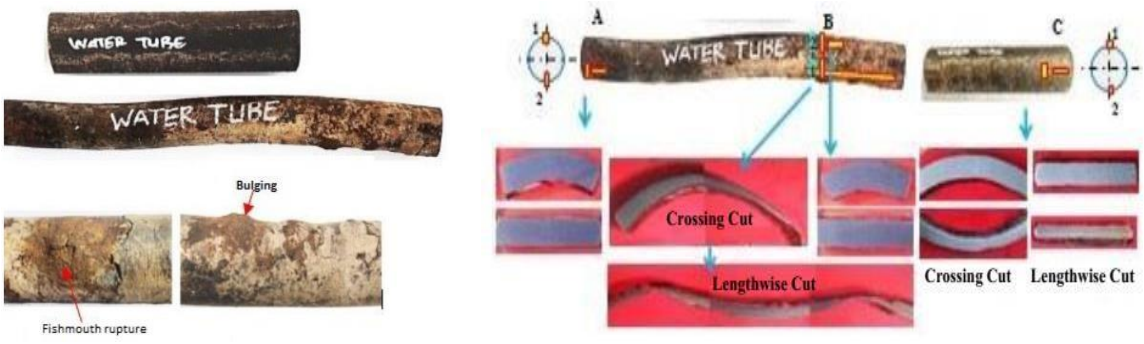

(a) **(b)**

Fig. 9 - Tubes on a fireside. (a) Tubes which show bulging at boiler tube surface of the firesid; (b) Sampling for an examination of the microstructure and hardness test on tubes

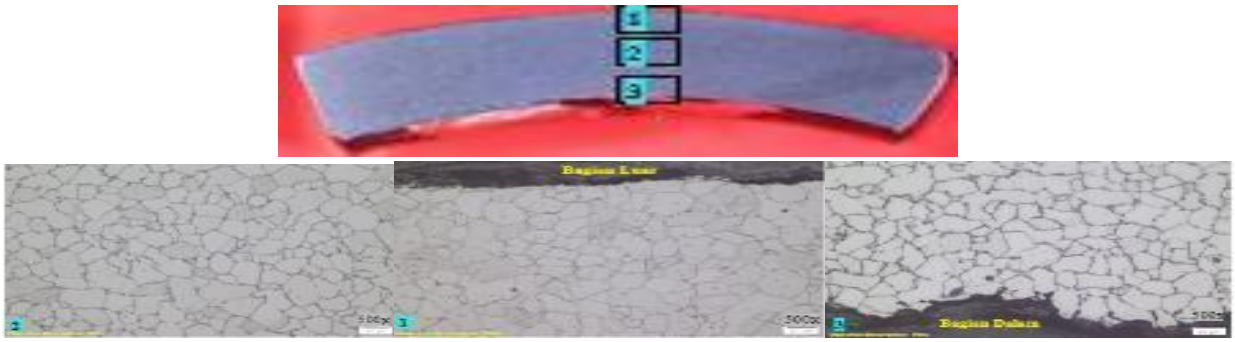

Location A: Sample 1 Crossing Cut

Fig. 10 - Microstructure location A sample 1 cross-section (locations 1, 2, and 3) in the form of ferrite (white) and pearlite, which has been transformed into pearlite spheroidization at grain boundaries. Etching: nital 2%.

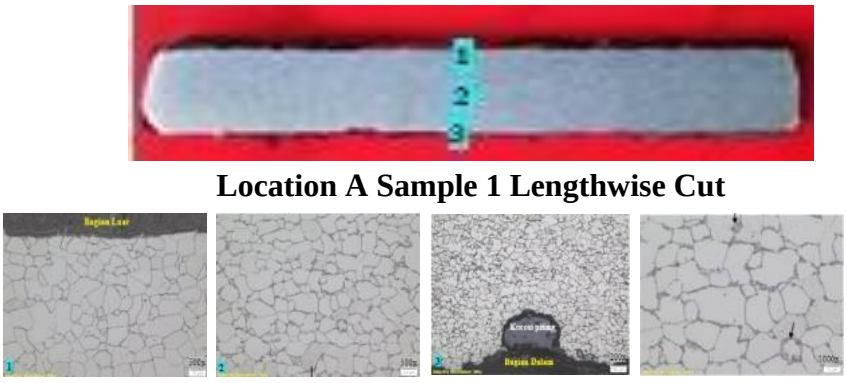

Location A Sample 1 Lengthwise Cut

Fig. 11 - Microstructure location A sample 1, lengthwise cut (locations 1, 2 and 3) in the form of ferrite (white) and pearlite which has been transformed into pearlite spheroidization at grain

boundaries. Etching: nital 2%.

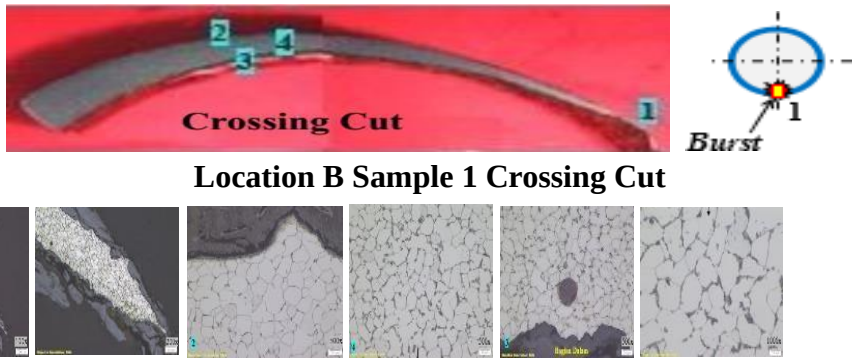

Location B Sample 1 Crossing Cut

Fig. 12 - Microstructure Location B sample 1 crossing cut (locations 1, 2, 3, and 4) in ferrite (white) and pearlite has been transformed into pearlite spheroidization at grain boundaries. Etching: nital 2%

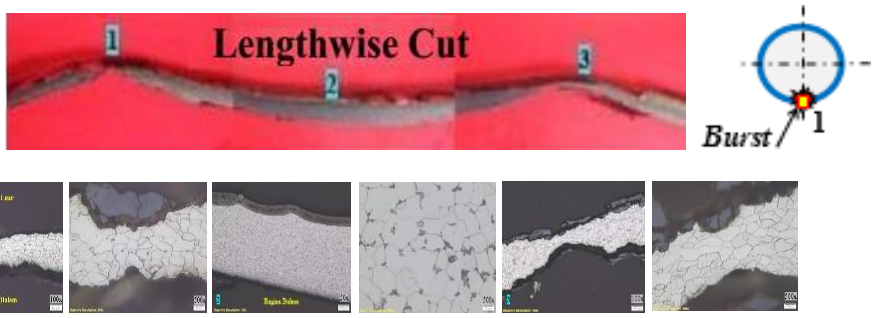

Location B Sample 1 Lengthwise Cut

Fig. 13 - The microstructure of Location B (burst location) sample 2 cross-sections (1 and 3) is ferritic and at location 2 is ferrite-pearlite which has turned into pearlite speroidization at the grain boundaries. Etching: nital 2%

Location B Sample 2, Cross Section

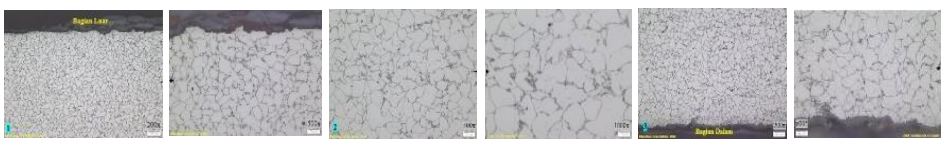

Fig. 14 - The microstructure of Location B (burst location) samples 2 crossing cut (1, 2 and 3) in

the form of ferrite and pearlite spheroidization at the grain boundaries. Etching: nital 2%

Location B Sample 2, Lengthwise Cut

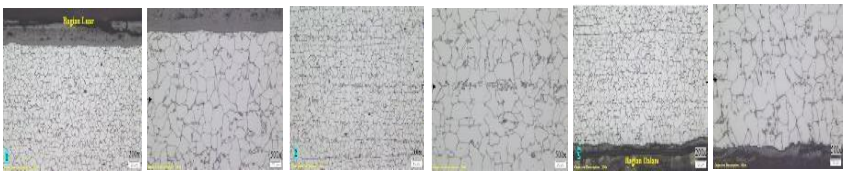

Fig. 15 - The microstructure of Location B (burst location) sample 2 lengthwise cut (1, 2 and 3) in the form of ferrite and pearlite spheroidization at the grain boundaries. Etching: nital 2%

Location C Sample 2, Cross Section

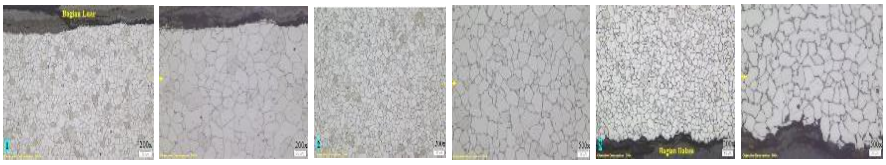

Fig. 16 - Microstructure Location C sample 2 crossing cut (1, 2 and 3) in the form of ferrite and pearlite spheroidization at grain boundaries. Etching: nital 2%

Location C Sample 1, Lengthwise Cut

Fig. 17 - Microstructure Location C sample 1 lengthwise cut of ferritic and middle part (2) and

inner part (3) of ferrite and pearlite spheroidization at grain boundaries. Etching: nital 2%.

Location C Sample 2, Crossing Cut

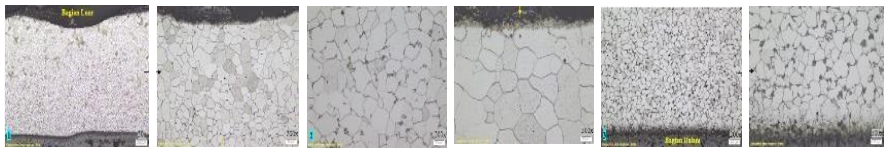

Fig. 18 - Microstructure Location C sample 2 crossing cut (1) in the form of ferritic and in the middle (2) and the inside (3) in the form of ferrite and pearlite spheroidization at the grain boundaries. Etching: nital 2%

Location C Sample 2, Lengthwise Cut

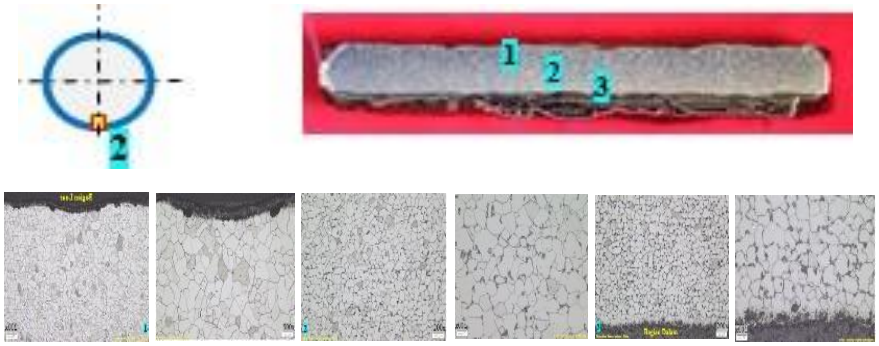

Fig. 19 - Microstructure Location C sample 1 lengthwise cut of ferritic and middle (2) and inner (3) of ferrite and pearlite spheroidization at grain boundaries. Etching: nital 2%

3.6. Analysis of Microstructure of Standard Tube Material

In Fig. 20 dan Fig. 21 showed the microstructure material of standard intact water tubes boiler (ASTM A213 T12). Samples 1 and 2 of the crossing cut and lengthwise cut (locations 1, 2 and 3) were ferrite (white) and pearlite (black). The intact tube shows have no degradation phase, so that it can be used as a reference to comparison.

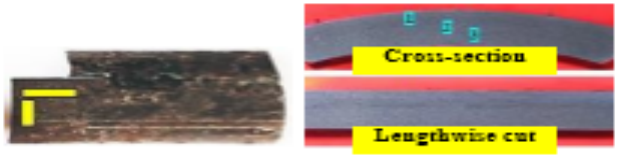

Standard material of Tube Sample 1

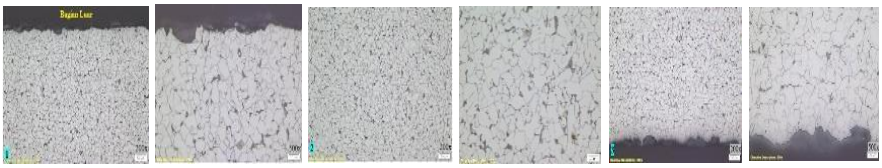

Fig. 20 - The microstructure of the normal sample tube 1 crossing cut (locations 1, 2 and 3) was ferrite (white) and pearlite (black). Etching: nital 2%

Standard Tube Material Sample 2

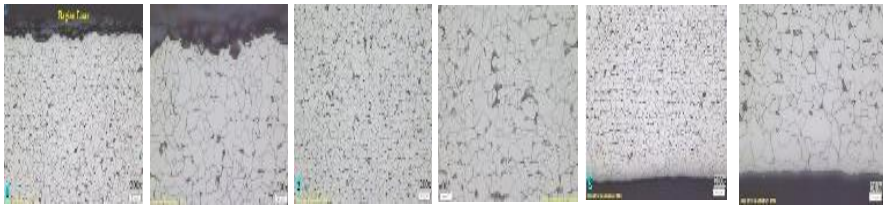

Fig. 21 - The microstructure of the normal sample tube 2 pieces lengthwise (locations 1, 2 and 3) in the form of ferrite (white) and pearlite (black). With fine grains resulting from the formation process. Etching: nital 2%

4. CONCLUSIONS AND SUGGESTIONS

4.1 Conclusions

Sequences of failure can be outlined as follows based on the study and conclusions made on the root cause:

a. The results of the analysis of visual observations showed that the boiler tube is damaged in the shape of a fish mouth. There has been overheating. This is an indication that there is overheating that can cause bulging during the operation in the tubes.

b. Results of hardness testing showed that ruptured tubes have lower hardness than the undamaged tubes. Under these conditions, the damaged tubes were softened (annealing). This is corroborated by the tensile strength testing results, which showed that ruptured tubes have a lower tensile strength than in the intact ones.

c. The chemical composition testing results of the tubes that failed experienced some element degradation, such as; C, Mn, Ni, Cr, Ti, Mo and Cu, which will reduce the physical and mechanical properties of the tubes' material.

d. Based on the results of tube crust analysis. The dominant elements in the crust/deposit inside and outside tube are solid that tends to form a crust precipitated calcium carbonate ($CaCO_3$), calcium

sulfate (CaSO4 .2H2 O), magnesium carbonate (MgCO3) and deposit of strontium sulfate (SrSO4) which has a low forming intensity, besides other scale deposits, such as iron carbonate (FeCO3) and iron sulfide (FeS).

e. The microstructure analysis results ruptured tubes change ferrite and pearlite become spheroidizing of pearlite at grain boundaries. On the contrary to the microstructure of intact tubes material, which was in the form of ferrite pearlite with a fine grain.

f. Overheating occurs as a result of heat transfer prevention in the tubes is inhibited in the presence of deposit (crust) either inside or outside of the insulator tubes.

4.2 Suggestion

It is necessary to research the phenomenon of deposits (scale) that occur both inside and outside the tubes. It is necessary to test the quality of the feed water (Feed Water Composition) used in the boiler operation process. It is necessary to analyze the quality of fuel (coal) to avoid corrosion on the boiler water tubes' outer surface.

Acknowledgments

The work carried out in the Water Tube Boiler Project-Based Learning Activities: Case Study at Textile Processing Plant, for which the first author would like to thank Bintang Adjiantoro, Mohd. Fuad Abdul Hamid and Muhammad Yunan Hasbi who has helped in completing this research.

Conflict of Interest

The authors declare no conflict of interest.

REFERENCES

[1] B. Haghighat-Shishavan, H. Firouzi-Nerbin, M. Nazarian-Samani, P. Ashtari, and F. Nasirpouri, “Failure analysis of a superheater tube ruptured in a power plant boiler: Main causes and preventive strategies,” Eng. Fail. Anal., vol. 98, no. January, pp. 131–140, 2019, doi: 10.1016/j.engfailanal.2019.01.016.

[2] U. Pal, K. Kishore, S. Mukhopadhyay, G. Mukhopadhyay, and S. Bhattacharya, “Failure analysis of boiler economizer tubes at power house,” Eng. Fail. Anal., vol. 104, no. January 2017, pp. 1203–1210, 2019, doi: 10.1016/j.engfailanal.2019.06.085.

[3] D. Sembiring, D. S. Widodo, B. Adjiantoro, A. B. Saman, and B. A. B. D. Kader, “Failure Analysis of the Furnace Scotch Boiler,” Int. J. Eng. Adv. Technol., vol. 9, no. 1, pp. 3697–3704, 2019, doi: 10.35940/ijeat.a9855.109119.Paresh Haribhakt et al., (2018). *Failure Investigation of Boiler Tubes a Comprehensive Approach*. ASM International Material Park, OH 44073-0002 www.asminternational.org

[4] Ahmad, J. et al., (2012). High Operating Steam Pressure and Localized Overheating of A Primary Superheater Tube. *Engineering Failure Analysis*, 26 (February 2011), pp.344–348.Available at: http://dx.doi.org/10.1016/j.engfailanal.2012.08.012.

[5] ASTM, (1996). E112: Standard Test Methods for Determining Average Grain Size. *West Conshohocken*, 96 (2004), pp. 1–26.Available at: http://scholar.google.com/scholar hl en&btnG Search & quintile: Standard Test Methods for Determining Average Grain Size 1.

[6] Koshy, M., (2015). Super Heater Tube Analysis for Oxide Scale Growth at Various Operating Conditions. *International Journal of Innovative Research in Science, Engineering and Technology*, 4(7), pp.6549–6553.

[7] Purbolaksono, J. et al., (2009). Failure Case Studies of SA213-T22 Steel Tubes of the Boiler through Computer Simulations. *Journal of Loss Prevention in the Process Industries*, 22, pp.719– 726. Available at: http://dx.doi.org/10.1016/j.jlp.2009.06.005.

[8] Rahman, M. & Kadir, AK, (2011). Failure Analysis of High-Temperature Superheater Tube (HTS) of a Pulverized Coal-Fired Power Station. *In Proceeding of the International Conference on Advanced Sciences, Engineering and Information Technology* 2011. pp. 517–522.

[9] Robert, PD & Harvey, H.M., (1991). *The Nalco Guide to Boiler Failure Analysis. Nalco Chemical Company*, New York, McGraw Hill Inc.

[10] Saha, A. & Roy, H., (2017). Failure Investigation of a Secondary Super-Heater Tube in a 140 MW Thermal Power Plant. *Case Studies in Engineering Failure Analysis*, 8 (May), pp.57–60. Available at: http://dx.doi.org/10.1016/j.csefa.2017.05.001.

[11] Sarisyuda, Bustamisyam & Indra, (2012). Failure Analysis of Super-heater Tube Boiler Package Due to Overheating. *Mekintek*, 3(1).

[12] Sukandar, (2002). Damage Analysis of Boiler Feed Water Tubes (BFW) at the end of the Injector Inhibitor Duct. *Thesis Report*, Machine Technology Magister FT-UI.

[13] Adrian et al., (2016). "Damage Analysis of Super-heater Tube Boiler Type ASTM A213 Grade T11 on "Steam Power Plant", *Engineering Journal ITS* Vol.5 No 2, pp. 148–152.

[14] Edwin Lim Chui Seng, (2013). *Evaluation of High-Temperature Boiler Tubes Using Iterative Analytical Approach*", Universiti Tunku Abdul Rahman, April 2013

[15] ASTM A213/A213M, (2019). "Standard Specification for Seamless Ferritic and Austenitic Alloy-Steel Boiler, Super-heater, and Heat Exchanger Tubes, *ASTM International*.

[16] M. Halim, S. Ismail, M. Kamal, and A. Aziz, (2009). "Review of Literature on Steam Accumulator Sizing in Palm Oil Mill", *European Journal of Scientific Research*, November 2009.

[17] ASTM E92, (1996). "Standard Test Method for Vickers Hardness of Metallic Materials", *ASTM International.*

[18] S.R. Lampman, (2004). ASM Handbook Volume 9, "*Metallography and Microstructures*"

[19] M. Nurbanasari & Abdurrachim, (2014). Investigation of Leakage on Water Wall Tube in a 660 MW Supercritical Boiler", Journal of Failure Analysis and Prevention, *Volume 14, No. 5, 2014.*

[20] *K. Singh, A.Chhabra & V. Kapoo*r, (2017). "Effect on Hardness & Micro Structural Behaviour of Tool Steel After Heat Treatment Process", *Scholarly Research Journal for Humanity Science & English Language*, 2017

[21] E. Karantzalis, A. Lekatou, and H. Mavros, (2009). "Microstructure and Properties of High Chromium Cast Irons : Effect of Heat Treatments and Alloying Additions", *International Journal of Cast Metals Research*, Vol.22, No. 6. December 2009.

[22] N. Srisuwan, K.Eidheh, N. Kreatsereekul, T.Ying Samphan Chareon, A. Kaewvilai, (2016). “The Study of Heat Treatment Effects on Chromium Carbide Precipitation of 35Cr- 45Ni-Nb Alloy for Repairing Furnace Tubes" *Journal Metals, MDPI*, no. 1, 2016.

[23] M. Asnavandi, M. Karam, M. Rezaei, and D. Rezakhani, (2017). "Fire-Side Corrosion : A Case Study of Failed Tubes of a Fossil Fuel Boiler Fire-Side Corrosion : A Case Study of Failed Tubes of a Fossil Fuel Boiler", *International Journal of Corrosion*, January 2017.

[24] W. Liu and W. Liu, (2015). "*The Dynamic Cree Rupture of a Secondary Superheater Tube in a 43 MW Coal-Fired Boiler by the Decarburization and Multilayer Oxide Scale Build-up on Both Sides,” Eng.* Fail. Anal.

[25] A.A. Khadom, A.A. Fadhil, A.M.A Karim, H. Liu. (2015). “Effect of Hot Corrosion on Boilers Tubes in North Baghdad Electric Power Plant Station”, *Diyala Journal of Engineering Sciences*, pp. 776– 784, 2015.

[26] D. W. Hoeppner and C. A. Arriscorreta, (2012). “Exfoliation Corrosion and Pitting Corrosion and Their Role in Fatigue Predictive Modeling : State-of-the-Art Review”, *International Journal of Aerospace Engineering.*